STUDY OF LITHIUM DOPED SOLAR CELLS

FINAL REPORT

June 11, 1969

JPL CONTRACT NO. 952250

Jet Propulsion Laboratory
California Institute of Technology
4800 Oak Grove Drive
Pasadena, California 91103

Prepared by

Peter A. Iles

Centralab Semiconductor Division
GLOBE-UNION, INC.

4501 N. Arden Drive
El Monte, California 91734

Study of Lithium Doped Solar Cells

Final Report

from

Centralab Semiconductor Division

under JPL Contract 952250

This work was performed for the Jet Propulsion Laboratory, California Institute of Technology, as sponsored by the National Aeronautics and Space Administration under Contract NAS7-100.

This report contains information prepared by Centralab Semiconductor, a Division of Globe-Union Inc., under JPL Subcontract.

Its content is not necessarily endorsed by the Jet Propulsion Laboratory, California Institute of Technology, or the National Aeronautics and Space Administration.

ABSTRACT

This year's work has led to improved control of all cell fabrication steps, allowing closer grouping of the cells shipped for irradiation. Better understanding was gained of the effects on cell properties caused by the different methods of silicon growth, and by the various lithium diffusion schedules. Continued efforts were made to find the best way to introduce lithium into the cells, by a method suited to scaling-up. The boron trichloride diffusion process appeared to affect cell properties far more than previously expected. Alternate boron diffusion methods showed promise, in allowing better evaluation of the various silicon crystal growth methods and also in enabling new structures to be made.

Two new cell structures were made. One structure combined an oxygen-rich layer on oxygen-lean bulk silicon. The oxygen layer should stabilize PN junction properties, while maintaining the rapid cell recovery given by the oxygen-lean bulk. The other structure had lithium introduced into the cells through the boron diffusion layer on the front surface.

Details of the cells shipped are given.

TABLE OF CONTENTS

LIST OF FIGURES

1.0 Introduction

The objective of this work is to develop high efficiency solar cells using lithium doping to improve cell stability in the charged particle environment in space. The method is to improve the fabrication processes for lithium solar cells, to test their potential for use as power sources, and to provide well controlled groups of cells with deliberately introduced variations for evaluation by various irradiation groups. A first requirement is to understand the pre-irradiation properties and then to relate these properties with the post-irradiation behavior.

This report surveys the basic cell fabrication steps, the introduction and distribution of lithium in the cells, and the effect of the lithium and the silicon properties on cell performance. Also described are some associated tests, the groups of cells shipped during the year, and trials of some different cell structures.

2.0 Basic Cell Fabrication Steps

2.1 Surface Finish: Tests have continued throughout the contract to improve the fabrication steps. Most cells have been made with a lightly etched, lapped finish slice, but good cells were also made from slices with a high optical finish.

2.2 Boron Diffusion: The P+ layer is produced by boron diffusion and mostly boron trichloride gas has been used as the source. This method is convenient and has produced high quality cells. However, there are several consequences of this gaseous process which restrict work in some of the areas described later. These consequences are the removal of ½ to 1 mil of silicon by boron trichloride etching, stresses introduced into the silicon by the boron layer, and the need for a hybrid antireflective coating because

the boron skin left on the silicon has different optical properties from ordinary highly doped P-silicon. In practice, the coating procedure can be adjusted to allow collected currents under AMO illumination as high as those measured in the best quality N/P cells. The gas etching complicates work where the P+/N cell must contain a thin layer to improve radiation properties (see 8.0 below). The stresses drastically increase the dislocation density of the silicon and prevent full evaluation of low dislocation density silicon. These stresses may also affect the behavior of lithium diffused into the silicon.

Because of these disadvantages of the BCl_3 process alternative boron diffusion methods were found which can produce good quality cells without the above disadvantages. More work is needed to build these methods into possible production processes.

2.3 Other Processes: In most cases, the PN junction produced for lithium cells is of good quality. The titanium-silver contacts have generally been adequate for use in the present program. Tests have been made on other contact metals, and of these aluminum has provided good cells. As expected, there were no difficulties in making lithium cells all or partly solder coated or of larger size.

3.0 Introduction of Lithium into the Silicon

Several methods have been studied. Some have shown promise in some aspects, but more work is needed to find the best overall method. The methods tried are as follows:

1. Paint-on using suspensions of lithium metal or compounds.

2. Thermal evaporation of lithium metal, either in high vacuum or at relatively high inert gas pressures.

3. Lithium Vapor transport.

3.1 Suspensions: Oil suspensions were used most. They are convenient and gave consistent cells, but they have several disadvantages. These disadvantages include a tendency for clusters of lithium metal to form deep pits by localized alloying, with great chance of breakage, and difficulty in covering the whole back surface of the slice. Full coverage could be obtained by depositing on a slice larger than the final cell and later shaping, but this is not as convenient as correctly shaping the starting slice.

A solution of lithium aluminum hydride in ether was obtained from TRW and tested. This solution gave reduced surface damage, maintaining the surface finish as it was before lithium diffusion. Better coverage near the edges was obtained but was still not complete. The lithium concentration at the surface and in the cell was slightly lower than that obtained from the oil suspensions but compensating changes in diffusion schedule can remedy this.

3.2 Evaporation: Vacuum evaporation has several theoretical advantages including a clean source, clean deposition conditions, control of the slice temperature during deposition, full coverage on the exposed surfaces and the possibility of shadow masking. However, practical difficulties were found. Sample heating during evaporation caused loss of lithium from the silicon, and this in turn led to a wide spread in the electrical characteristics of the cells, even if the diffusion was performed outside the vacuum system in an inert atmosphere. Cover layers evaporated over the lithium did not reduce the loss of lithium. Lately, improved evaporation boat design and procedures have given more consistent cells. The main remaining defect is that lithium vapor leaks to the front surface of the cell, either degrading the antireflective coating or, in extreme cases, degrading the P+ layer or contacts.

A variant of evaporation used relatively high vapor pressures (50 micron Hg) of argon between the lithium source and the samples. The main defect was uneven lithium distribution from gas flow

patterns, and no advantage was found in this method.

For all these deposition methods the carrier gas used during diffusion affected cell properties. Although more inert gases did not give greater surface concentration of lithium, they allowed more interaction between the lithium and the silicon often increasing the cell breakage.

3.3 Lithium Vapor Transport: In this, lithium metal was heated to above 700° C, and an argon stream carried the vapor down a furnace tube over silicon slices held at the diffusion temperature. Several practical difficulties resulted. Lithium vapor was very reactive, necessitating great care in the choice and coverage of the furnace lining, and the gas flow patterns gave uneven lithium coverage. The lithium vapor reacted with all surfaces of the silicon, and this was a disadvantage if the attack degraded the front surface components of the cell. However, it was also possible with this method to introduce lithium into the cell through the front surface P+ layer (see 8.3 below). The vapor method in principle could provide controllable (and lower) surface concentrations.

SUMMARY

Paint-on methods have consistently produced closely controlled cell characteristics for all the ingots used. The lithium aluminum hydride suspension avoids several of the faults of the oil suspensions and is undergoing more thorough evaluation.

Vacuum evaporation still shows promise for large scale use.

4.0 Distribution of Lithium in Cells

The amount and concentration gradient of lithium in the cells can affect cell properties before and after irradiation. Before irradiation more lithium near the PN junction reduced short circuit

current and the series resistance. More lithium near the back surface increased open circuit voltage up to about 600 mV. After irradiation, the amount of lithium affected the speed of recovery and the ability to recover after more severe fluences. The gradient of lithium near the PN junction controls cell stability. It is convenient to divide the various combinations of diffusion temperature and time into three classes:

4.1 Tack-on: Here the diffusion cycle is not severe, and a thin layer of lithium several mils deep is formed.

4.2 Drive-In: The diffusion cycle is more severe, and the lithium source is maintained in contact with the silicon. A deep layer heavy with lithium forms through most of the slice.

4.3 Redistribution: After either of the above cycles, the slices are cooled, the excess lithium is removed from the back surface, and the slice receives another diffusion cycle.

If redistribution follows a tack-on cycle, the profile changes as shown in Figure 1. If redistribution follows a drive-in cycle, the profile changes are as shown in Figure 2.

Some redistribution cycles produced fairly uniform concentrations. However, there was generally loss of lithium near each surface of the slice. The measured concentration gradient near the back surface appeared to be the result of out-diffusion. The loss near the PN junction may have been dissolution of lithium in the diffused boron layer. If a summation of the measurable donors was made after various redistribution cycles (by integrating under a linear plot of concentration versus distance) serious overall losses in lithium were found. Typically for 30 minutes redistribution at 450^{o} C, the amount of lithium fell by 70% for CG silicon, and by 40% for FZ silicon. Examination of the profiles in Figures 1 and 2 showed that most cycles gave lithium concentrations above 10^{15} cm^{-3},

thus converting most of the bulk N-silicon to low resistivity (< 1 ohm - cm) silicon.

It has been found that greater amounts of lithium near the PN junction reduce Isc (see Figure 3). Figure 4 shows that the Isc changes after various redistribution cycles could be explained by the changes in lithium concentration shown in Figures 1 and 2. Voc values were much less sensitive to these cycles.

4.4 Other Distributions: Diffusion at 600° C for 5 or 20 minutes gave low Isc. Redistribution cycles increased Isc, but it was still low.

Two groups of N-silicon were given a tack-on and a drive-in lithium diffusion respectively. They were then taken through the standard BCl_3 diffusion, this corresponding to a very severe redistribution cycle. Measurements showed only the starting background level of donors, and the cells made from these two groups showed that the short circuit current of the cell had not been degraded at all by the introduction and loss of lithium. Cells with above 31 mW output were obtained.

5.0 Influence of Silicon Crystal Growth Method

Three major methods of growing silicon crystals result in the properties shown in Table I.

TABLE I

Properties of Silicon Grown by Different Methods

Method	Maximum Resistivity (ohm-cm)	Dislocation Density (cm-3)	Oxygen Content (cm-3)
CG	100	Low-Medium (104)	High ($\sim 10^{18}$)
FZ	1000	High ($> 4 \times 10^4$)	Low ($< 10^{16}$)
Lopex, Monex	1000	Very Low ($< 10^2$)	Low ($< 10^{16}$)

Several separate tests have shown that if slices of the three growth variants were given identical BCl_3 diffusion, antireflective coatings and lithium diffusion, there was a consistent difference in the I-V properties of the cells. Generally the oxygen-lean silicon cells were similar but all differed from the oxygen-rich CG silicon. Table 2 summarizes the differences.

TABLE 2

Comparison of I-V characteristics for various kinds of silicon
(AMO, 140 mW/cm^2, cells 2 cm^2)

Lithium Diffusion Schedule	Monex, Lopex or FZ Silicon					CG Silicon				
	Isc mA	Tungsten only mA	Xenon only mA	I_{450} mA	Voc mV	Isc mA	Tungsten only mA	Xenon only mA	I_{450} mA	Voc mV
425°-90 min	54.5	30	25	51	560	63	38	25	57.5	590
425°-90 (+60) min	59.5	34	28	55	555	65	40	25	60	590
425-90 (+120)	65	37	28	53	550	68.5	43	27	65	585
450-40 min	55	28	28	50	560	63	37	26	59	600
450-40 (+80)	63.5	36	29	57	550	69	42.5	26.5	65	580

Figure 5 compares the whole I-V curves, Figure 6 the dark forward diode characteristics, and Figure 7 the ln Isc-Voc plots for various light levels. Voc did not vary much with diffusion cycle within each material type, and the difference between types was consistent. I_{sc} depended more on the diffusion cycle, the differences becoming less pronounced for longer redistribution times. Measurement of the lithium concentration in the two groups of materials did not explain the differences. Generally CG silicon had more lithium through the cell for an equivalent cycle, and this should have decreased I_{sc}. These material comparisons are being repeated using different boron diffusion methods to ensure that the dislocation density of the cells is close to that in the starting silicon.

At present none of the obvious material differences provide a clear explanation of the observed differences in the cells.

6.0 Associated Tests

6.1 Etch Pits: After etching to develop etch pits, the surface to which the lithium was applied had a "lumpy" appearance possibly caused by localized alloying. Often the etch pit density was lower where the lithium was, but it was possible that this was caused by a reduced preferential etch rate rather than by interaction of lithium and the dislocations.

6.2 Breaking Tests: Slices approximately 14 mils thick were center loaded until they broke. Although the breaking weights showed spread, possibly because of variable surface effects, three conclusions were possible:

1. Lithium diffusion alone did not markedly decrease the strength, although it increased the spread.

2. BCl_3 decreased the breaking weight.

3. Lithium added to BCl_3 diffused slices did not alter the values obtained in 2.

6.3 Oxygen Concentration: Infrared absorption at 9 microns was used to compare the oxygen content of various CG ingots, and also to search for a diffused oxygen layer in work described in Section 8.2 below.

6.4 Test for Shelf Drift: Over a three month period, tests on unirradiated cells showed that CG cells remained stable, a few Lopex cells were also steady, but cells made from FZ silicon degraded.

FZ cells which had a drive-in diffusion showed decreases of 6.5mA at I_{sc}, 25mV at Voc, and 6.5mA at I_{450}.

For FZ cells with a moderate redistribution cycle, I_{sc} remained stable, Voc fell by 15mV, and I_{450} decreased 10.5mA. This latter degradation may have been caused by changes in contact resistance.

7.0 Centralab Cell Shipments

To date seven shipments have been made and the eighth is in preparation. Over 1200 slices were processed to form these shipments, and each group was analyzed to show the cumulative yield obtained. The shipment details are given in Table 3, and the yields are shown in Figures 8, 9, and 10.

TABLE 3

Details of Cell Shipments

Shipment	No. of Cells	Si	Resistivity	Dopant	Li Diffusion	Avge AMO I-V values			
						Isc mA	I_{450} mA	P_{450} mW	Voc mV
C 1	60	CG	30	As	450-5 (+40)	70.5	67.5	30.5	60(
C 2	60	CG	10	Sb	425-90 (+120)	69.5	67.5	30.5	59(
C3	30	FZ	65	P	350-30	70	57.5	27	55(
	30	FZ	65	P	425-5	71	54.5	24.5	55(
C 4	12	Monex	100	P	425-90	54	50	22.5	56(
	12	Monex	100	P	425-90 (+60)	59.5	54	24.5	55
	12	Monex	100	P	425-90 (+120)	65	53	24	55
	12	Monex	100	P	450-40	55	50	22.5	55
	12	Monex	100	P	450-40 (+80)	63.5	56.5	25.5	55

Shipment	No. of Cells	Si	Resistivity	Dopant	Li Diffusion	Avge AMO I-V values Isc mA	I_{450} mA	P_{450} mW	Voc mV
C 5	30	CG	30	As	450-40	62	59	26.5	605
	30	CG	30	As	425-90 (+120)	69	64.5	29	585
	30	FZ	90	P	450-40	54	49	22	570
	30	FZ	90	P	425-90 (+120)	62	49	22	540
C 6	40	CG	3-16	Sb	425-90 (+120)	68	63	28.5	585
	40	CG	17-85	Sb	425-90 (+120)	68.5	63	28.5	585
	40	CG	16-57	P	425-90 (+120)	69	63	28.5	585
C 7	30	FZ	90	P	450-10	62	55.5	25	550
C 8	10	FZ	100	P	400-120 min				
	10	Lopex	90			$+O_2$ - skin			
	5	FZ	100	P	400-120 min				
	5	Lopex	90						
	10	FZ	100	P	400-10 min				
	10	CG	30	As		front and back surface			
	5	FZ	100	P	400-120 min				
	5	CG	30	As		back surface only			

7.1 Comments on Shipped Cells: C-1 cells were lightly doped with lithium and did not show good recovery. C-2 had moderate lithium doping but showed no recovery at room temperature. To test if the use of antimony as the starting dopant was the reason for this lack of recovery, group C-6 was fabricated. If antimony does not prove to be the reason, other possibilities such as a higher oxygen content in the ingot used for C-2 will be explored.

Groups C-3 and C-7 used short tack-on cycles to leave the active region of the cell without lithium. These cells were then subjected to a sequence of irradiation dosages and redistribution cycles at 250^{o} C, with monitoring of the cell performance. This enabled the degradation and recovery processes to be followed as lithium was progressively moved into the active region.

Group C-4 used Monex silicon and a progressive sequence of lithium distributions. Their behavior under irradiation by 0.7 Mev electrons is shown in Figure 11, and can be summarized as follows:

1. For all lithium doping levels, the degradation under fluences of 10^{14}, 5×10^{14}, or 3×10^{15} electrons/cm^2 was more severe for cells with lower lithium concentration near the PN junction. This difference in degradation may result from different annealing rates before the post-irradiation measurements.

2. The degree of recovery of maximum power was most complete as follows:

   a. for low fluence, for cells with light lithium doping.
   b. for medium fluence, for cells with medium lithium doping.
   c. for high fluence, for cells with heavy lithium doping.

8.0 Different Cell Structures

Some structures differing from the conventional lithium cell are worth consideration, either to improve cell

performance or to help understand the controlling processes.

8.1 P+N+N Configuration: This structure has already provided lithium cells with greater stability after heavy fluences. The PN junction is formed at the N+ layer after boron diffusion, and this junction remains stable despite large decreases in lithium concentration near the junction. Work continues to improve the starting performance of cells made with this structure.

8.2 Oxygen Layer Structure: Oxygen-lean silicon generally gives lithium cells with the fastest recovery after irradiation; however, the same silicon can allow most instability after recovery. Oxygen-rich silicon gives the opposite behavior, namely slower recovery with good stability. Because the recovery processes depend on the silicon properties in the bulk of the cell, whereas instability depends more on the properties close to the PN junction, a structure with a thin oxygen-rich layer at the front surface of a cell formed from oxygen-lean silicon seems worthy of study.

The fabrication sequence is shown in Figure 12. An oxygen-rich layer approximately 1 mil thick is formed by diffusion in an oxidizing atmosphere. A P+ layer is formed, preferably without removal of any of the oxygen layer. Contacts and coating are applied to this P+ layer, and then lithium is diffused in from the back surface. Finally the back contact is applied.

Some cells with this structure have already been made and such cells will form half the eighth shipment. The most encouraging result to date has been the surprisingly high quality of the bulk silicon after the severe oxygen diffusion schedule. Cells with output as high as 27mW have been obtained for Lopex and CG silicon, using moderate lithium doping.

A modification of this structure, close to that described in 8.1 above, is also being investigated. Here the oxygen layer is formed and is then converted to a donor-rich layer by heat treatment at 450° C.

If successful, these oxygen layer structures should provide valuable information on the defect-lithium-oxygen interactions.

8.3 Front Surface Introduction of Lithium: The usual procedure, introducing lithium from the back surface of the cell, is convenient, but has some disadvantages. First, a fairly severe diffusion cycle is needed to build up sufficient concentration of lithium in the active part of the cell near the front surface and often attempts to increase the concentration in this region leaves the rest of the body of the cell with excess lithium, or with severe concentration gradients. Second, the indiffusing lithium front has a gradient (often large) near the PN junction, and this may lead to unstable cell behavior.

At present no P+ formation methods have been found which can produce good lithium cells on silicon already diffused with lithium near the front surface.

Diffusion of lithium through an already formed P+ layer on the cell front can avoid some of the shortcomings of the usual method, but may in turn lead to other problems. These new problems are that it has proven difficult to diffuse lithium through the front surface with contacts and coating already formed, and if the contacts and coating are applied after lithium diffusion, the range of contact firing treatments is limited. Also, should the lithium build up concentration in small areas, it is possible to degrade the PN junction seriously.

Despite the difficulties, some cells have been made by diffusing lithium through the front surface, and some cells of fair quality have resulted. Using a short cycle of 400^{o} C for 10 minutes, more than 10^{16} lithium atoms per cm^{3} can be provided throughout the cell, and the following I-V values were obtained: Isc ~60 mA, Voc ~590 mV, I_{450} ~56 mA corresponding to P_{450} = 25 mW.

Measurements show there is still a slump in the measured lithium in the first few mils of the cell (see Figure 13). However, the lithium distribution is sufficiently different to warrant some irradiation tests on cells of this structure.

If successful, this structure could be effective for high fluences. Half the eighth shipment included these front surface introduction cells.

Front surface introduction of lithium can be combined with the various boron diffusion methods or with the structures described in 8.1 or 8.2.

8.4 Partial Compensation of P-Silicon: More attempts were made to controllably dope low resistivity P-silicon to around 10 ohm-cm by lithium diffusion. Success depends on getting lower and controllable lithium concentration, with low gradient throughout the P-silicon. Now more control exists on lithium introduction methods, this structure is worth trying again.

9.0 Conclusions

This year's work has seen consolidation and improvement of fabrication processes with more flexibility, allowing a wider range of structures to be tested. More understanding and control of the lithium distribution in cells has been achieved. More emphasis was directed toward crucible grown silicon, because previous work indicated that for real-time space conditions on many missions, the slower rate of recovery could be tolerated in order to gain the advantage of greater initial output and general stability. Closer examination of results on crucible grown silicon ingots shows that there is still need for closer control of the properties of these ingots.

Crucible grown silicon cells with lithium recover very well with only slightly accelerated annealing (80^{o}-100^{o} C) and thus show good promise now for missions where this forced annealing can be provided.

Oxygen-lean silicon still has advantages in fast recovery at room temperature, but seems to suffer from possible instability. However, more study is needed because understanding of the deficiencies in this material can be gained more quickly on the shortened time scale, and complete the overall picture of lithium cells. Some of the more complex structures are of help in understanding, but the goal now is to try and develop the "conventional" lithium cell into a useable space component.

10.0 Recommendations for Future Work

The section above has listed the promise of further improvements in lithium doped solar cells. The main features requiring attention are:

10.1 Closer control of the properties of crucible-grown silicon which affect cell performance.

10.2 Evaluation of a wider range of boron diffusion methods, in particular to check if the differences in cells made from oxygen-lean silicon are caused by real material differences or by interaction of the fabrication steps.

10.3 Continued study of lithium introduction methods to improve consistency.

10.4 Continued improvement in cell consistency, and examination of methods best suited to sealed-up production.

10.5 Fabrication of specified cells for use in the associated radiation test programs. Inclusion of realistic flight tests.

10.6 Use of greater control and flexibility in processing cells to provide novel structures to elucidate the mechanism underlying cell behavior.

11.0 New Technology

Most of the work described this year can be considered as application or combination of prior technology. However, the two structures described in Sections 8.2 and 8.3 can perhaps be classified as New Technology. Details have been filed separately with JPL.

Figure 1 Lithium concentration profiles following redistribution of a tack-on diffusion.

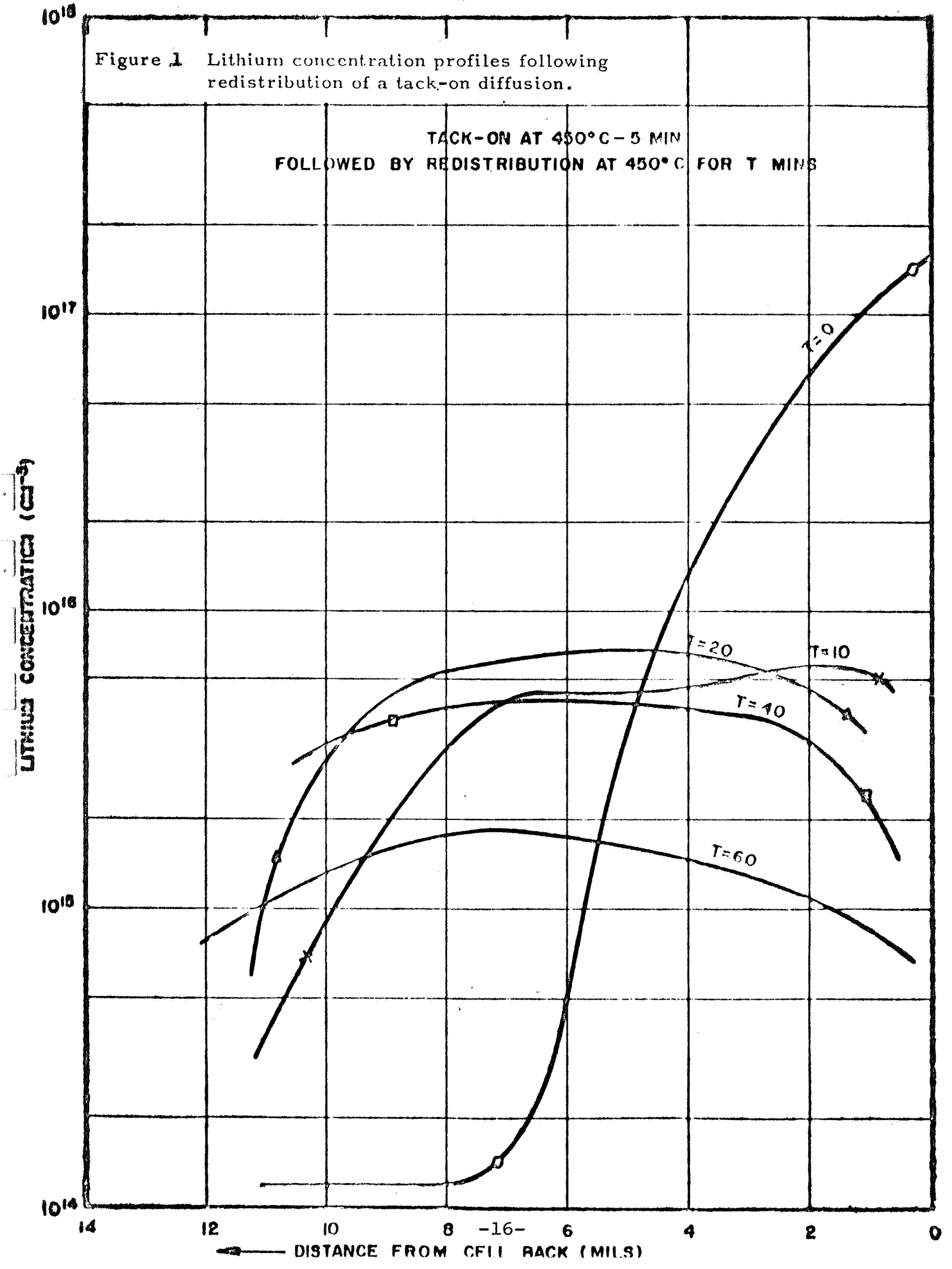

Figure 2 Lithium concentration profiles following redistribution of a drive-in diffusion.

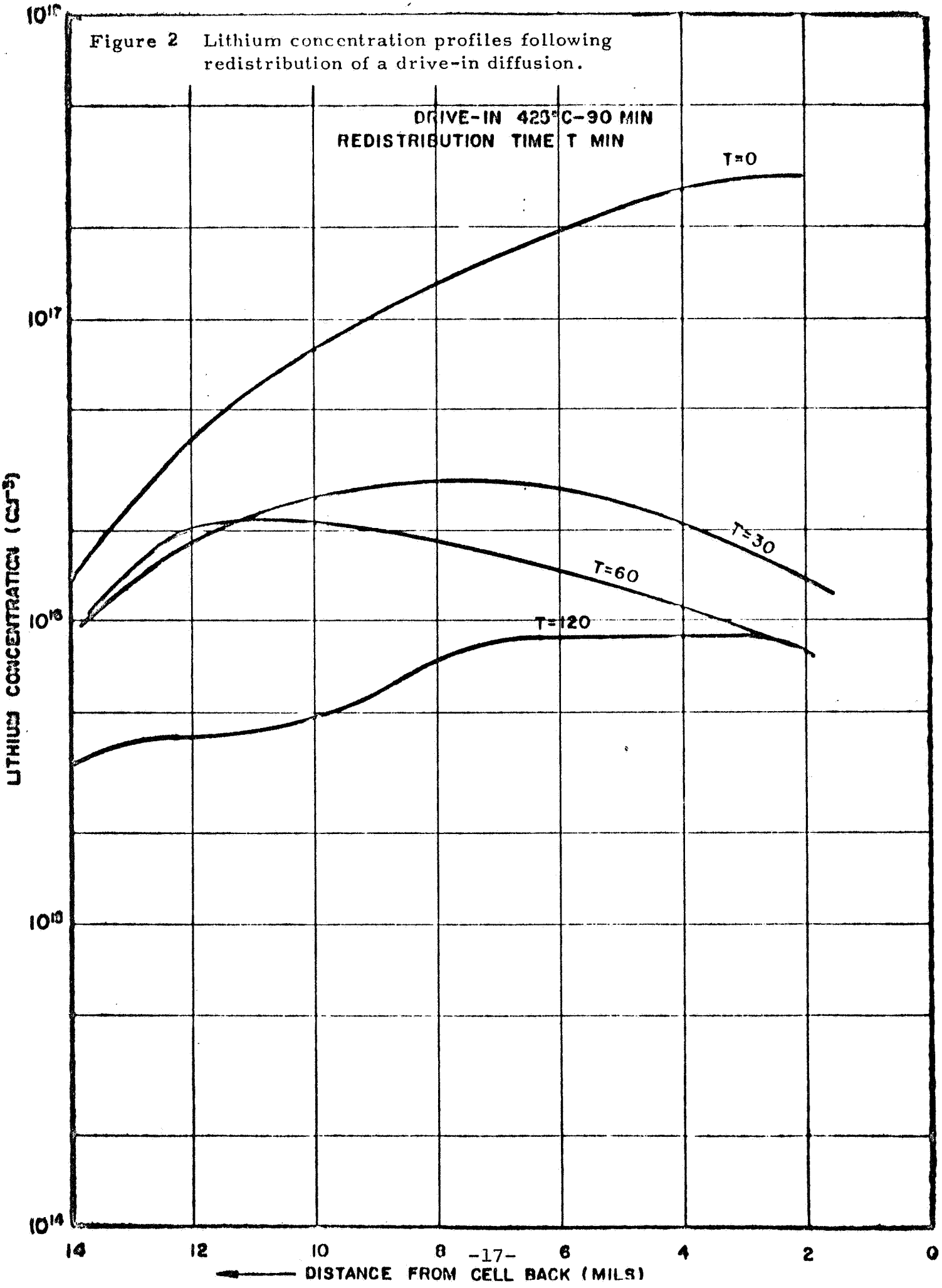

Figure 3 Isc versus lithium concentration near the PN junction. Cell area 2cm^2, space sunlight 140 mw/cm^2.

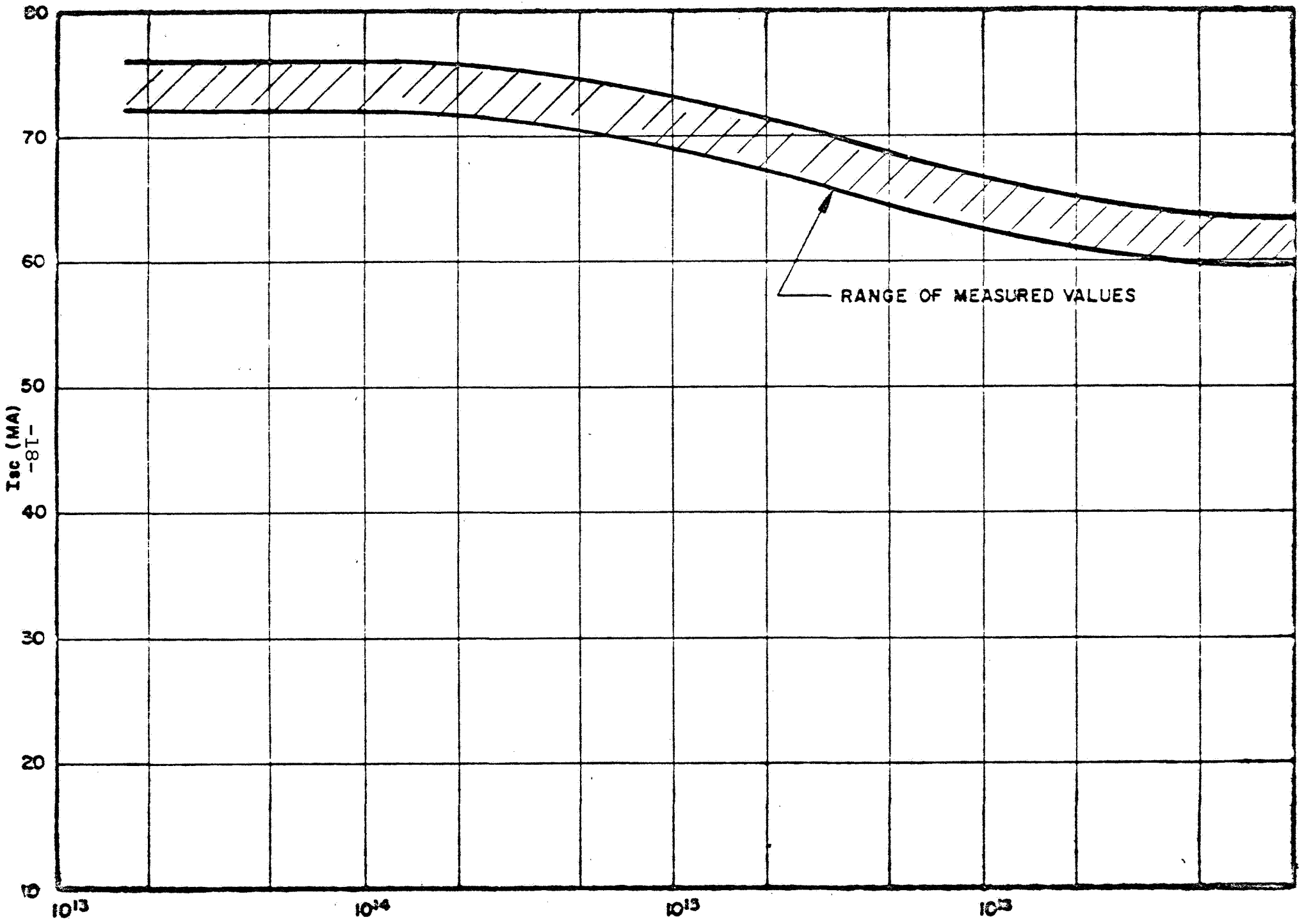

Figure 4 Isc as a function of redistribution time following either tack-on or drive-in lithium diffusion. Cell area 2cm^2, space sunlight 140 mw/cm^2.

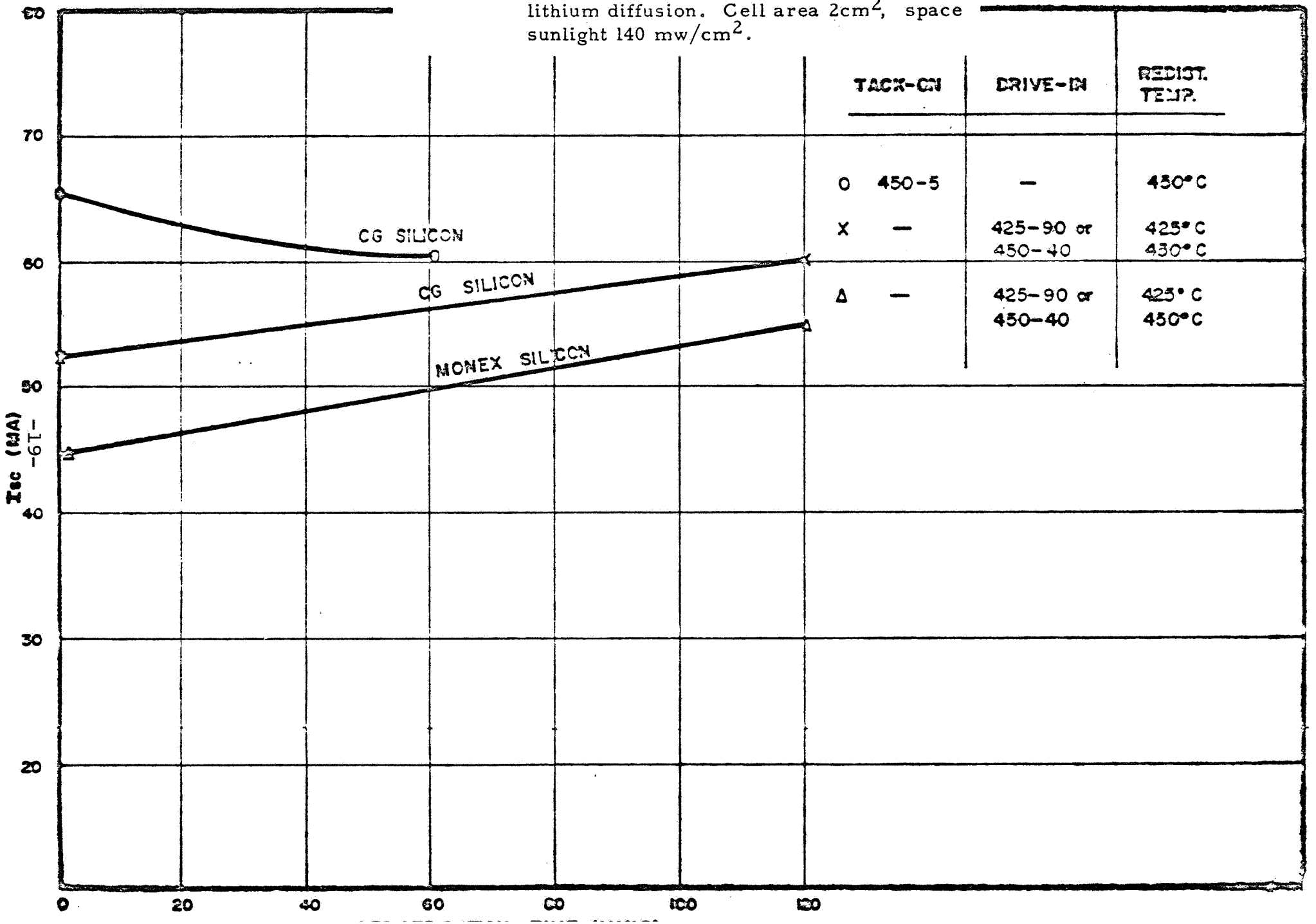

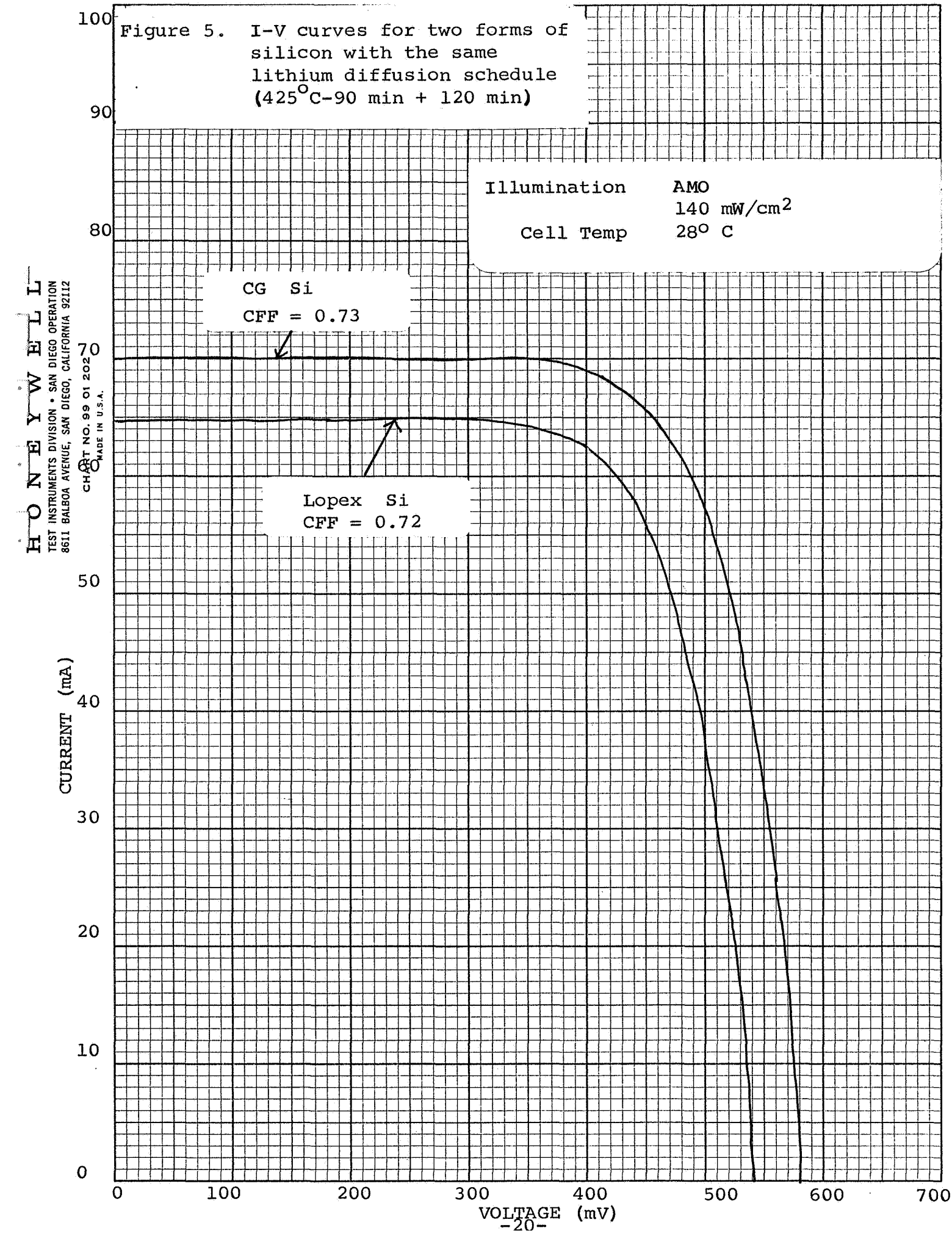
Figure 5. I-V curves for two forms of silicon with the same lithium diffusion schedule (425°C-90 min + 120 min)
Illumination AMO
140 mW/cm2
Cell Temp 28° C
CG Si
CFF = 0.73
Lopex Si
CFF = 0.72
CURRENT (mA)
VOLTAGE (mV)
0
10
20
30
40
50
60
70
80
90
100
0
100
200
300
400
500
600
700
HONEYWELL
TEST INSTRUMENTS DIVISION • SAN DIEGO OPERATION
8611 BALBOA AVENUE, SAN DIEGO, CALIFORNIA 92112
CHART NO. 99 01 202
MADE IN U.S.A.

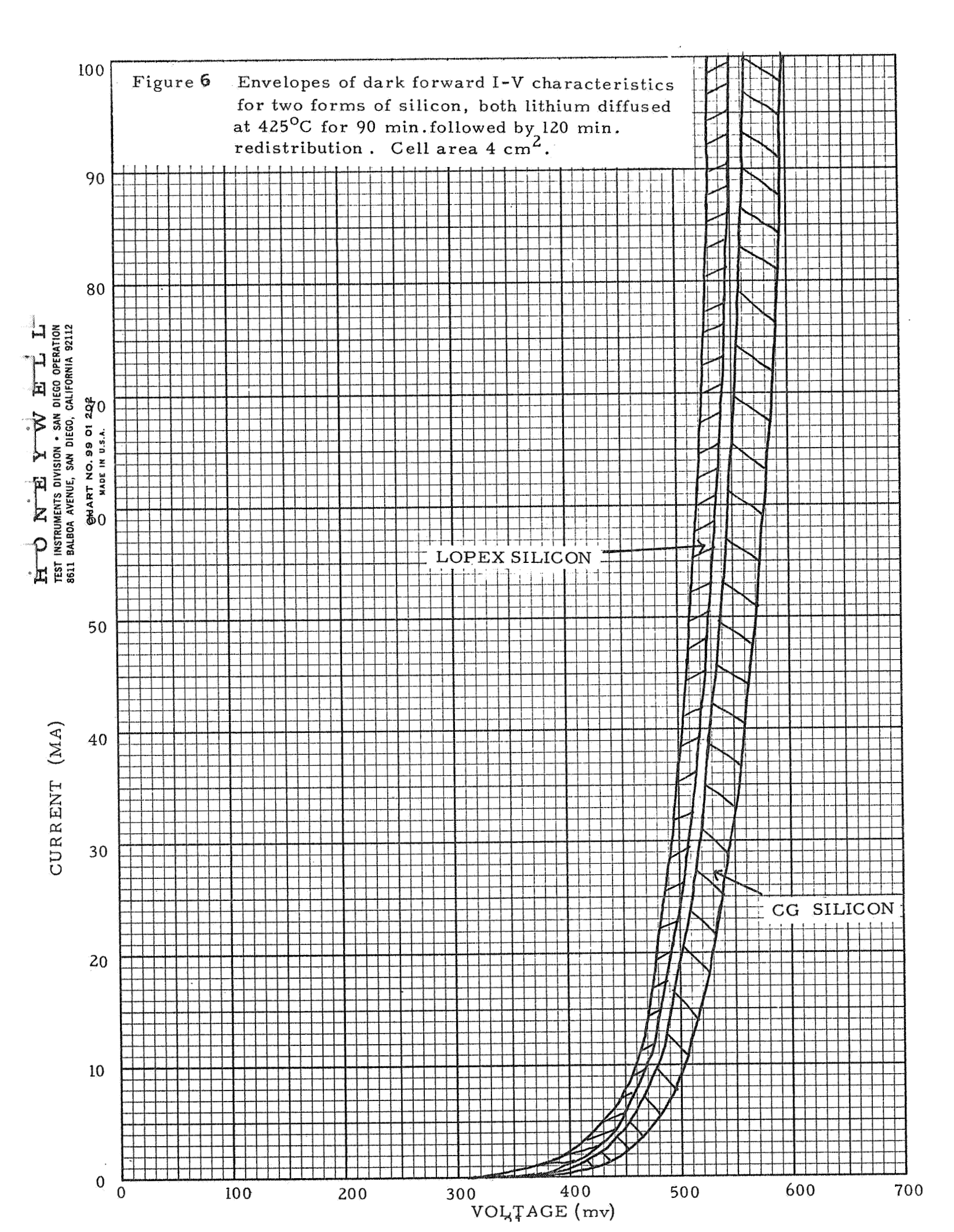
Figure 6 Envelopes of dark forward I-V characteristics for two forms of silicon, both lithium diffused at 425°C for 90 min. followed by 120 min. redistribution. Cell area 4 cm².
LOPEX SILICON
CG SILICON
CURRENT (MA)
VOLTAGE (mv)
0
10
20
30
40
50
60
70
80
90
100
0
100
200
300
400
500
600
700
HONEYWELL
TEST INSTRUMENTS DIVISION • SAN DIEGO OPERATION
8611 BALBOA AVENUE, SAN DIEGO, CALIFORNIA 92112
CHART NO. 99 01 202
MADE IN U.S.A.

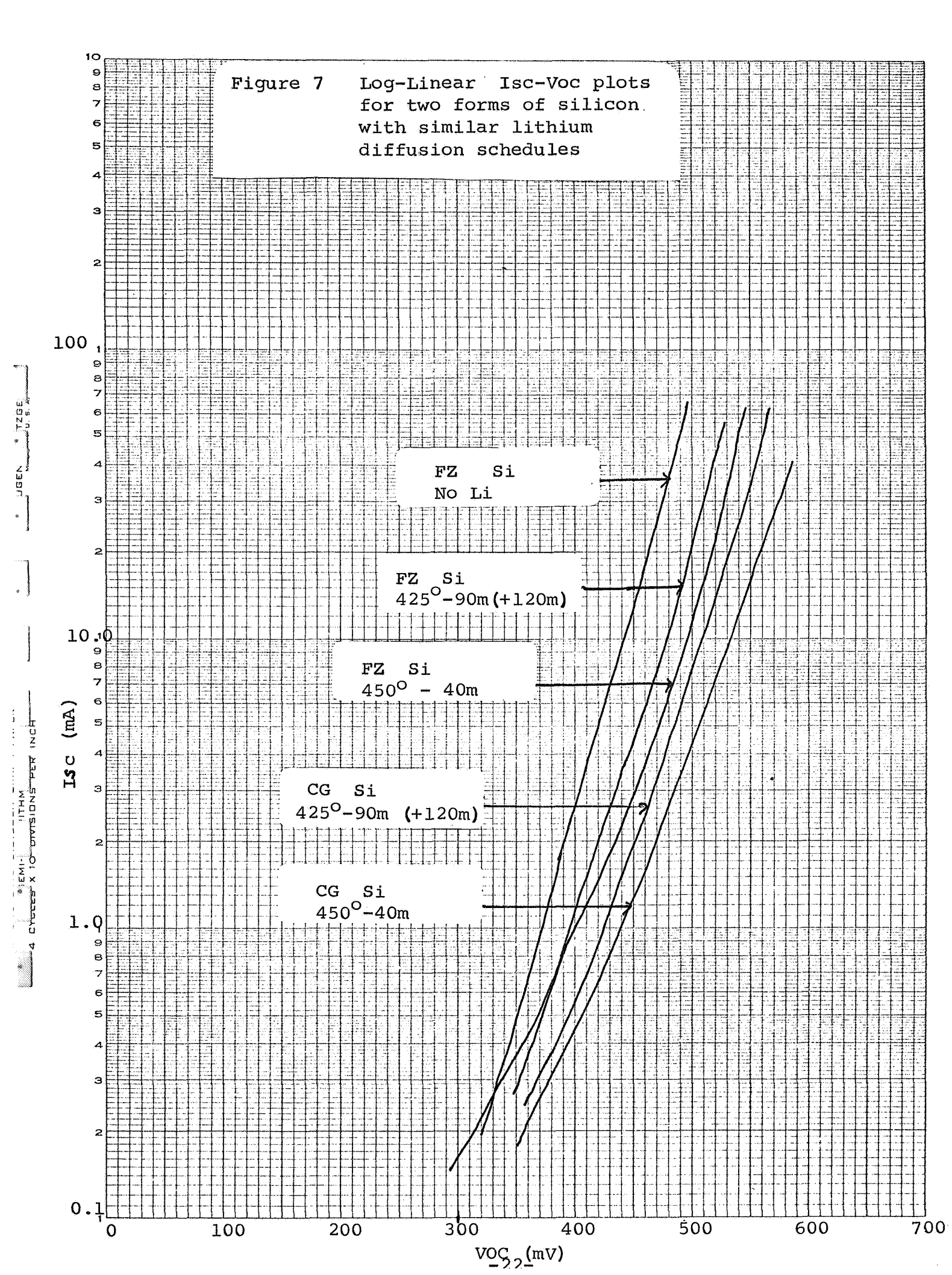
Figure 7 Log-Linear Isc-Voc plots for two forms of silicon with similar lithium diffusion schedules
FZ Si
No Li
FZ Si
425°-90m(+120m)
FZ Si
450° - 40m
CG Si
425°-90m (+120m)
CG Si
450°-40m
Isc (mA)
100
10.0
1.0
0.1
0
100
200
300
400
500
600
700
VOC (mV)

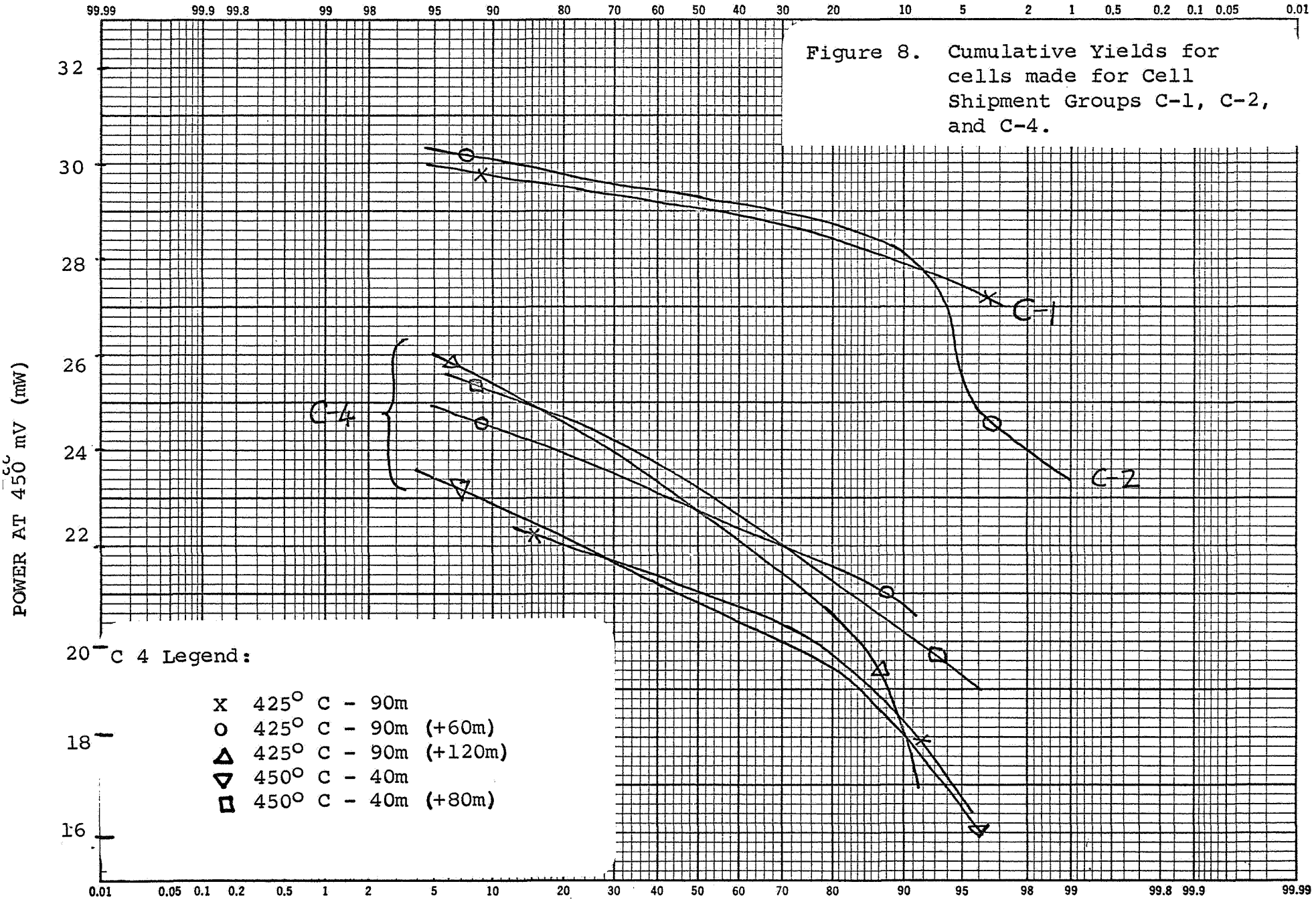

Figure 8. Cumulative Yields for cells made for Cell Shipment Groups C-1, C-2, and C-4.

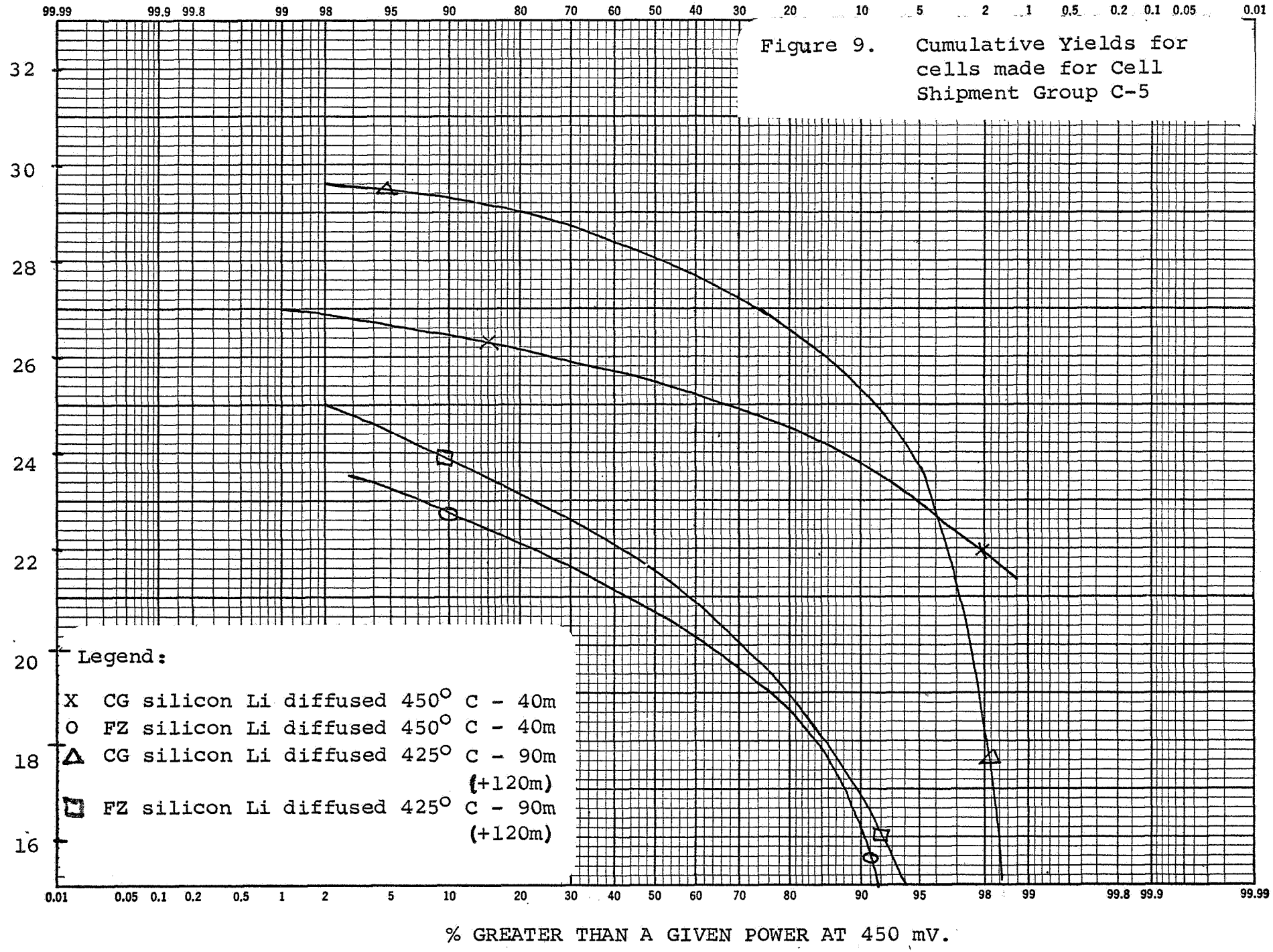

Figure 9. Cumulative Yields for cells made for Cell Shipment Group C-5

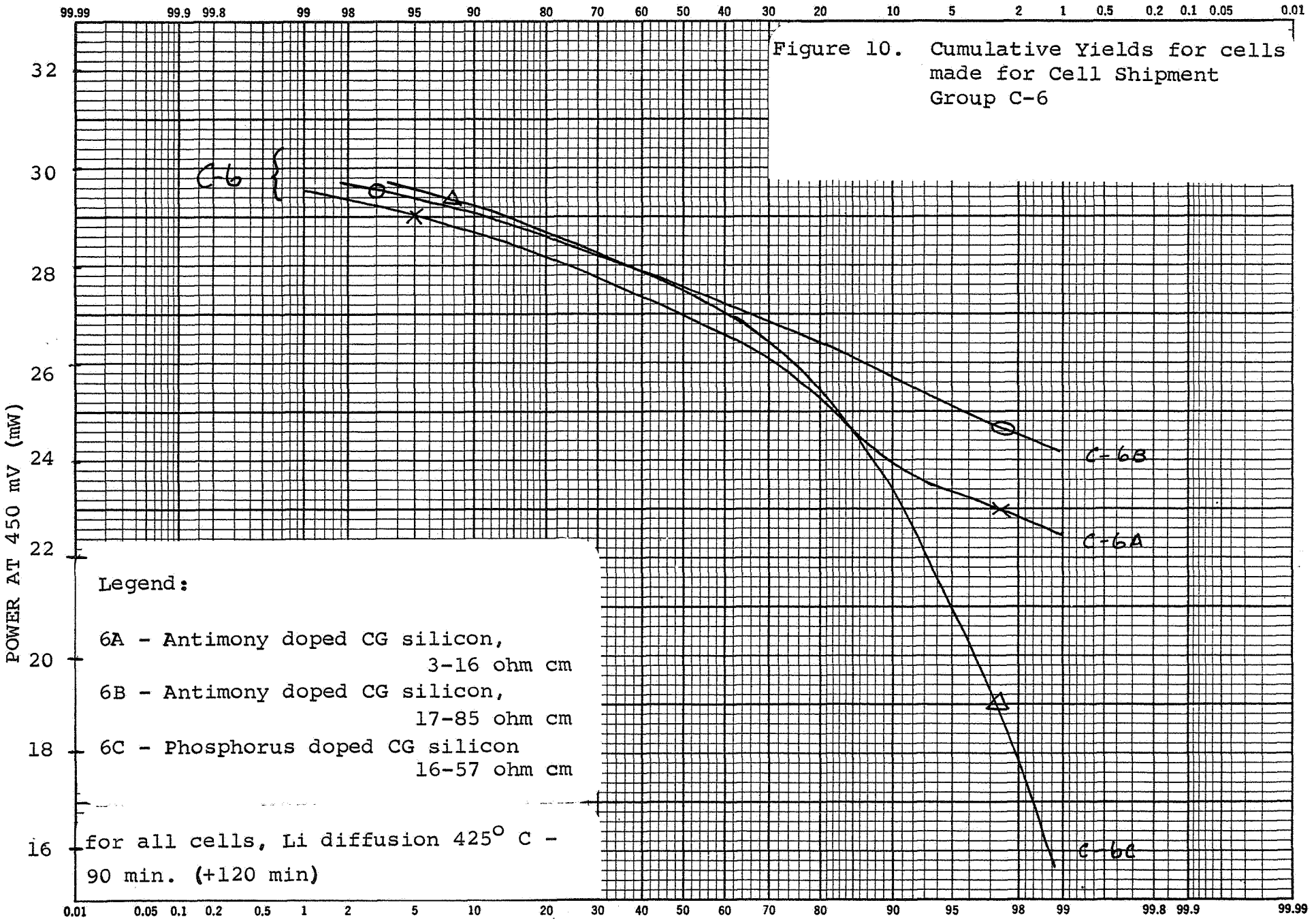

Figure 10. Cumulative Yields for cells made for Cell Shipment Group C-6

Figure 11 P/PO for 5 groups of C-4 cells

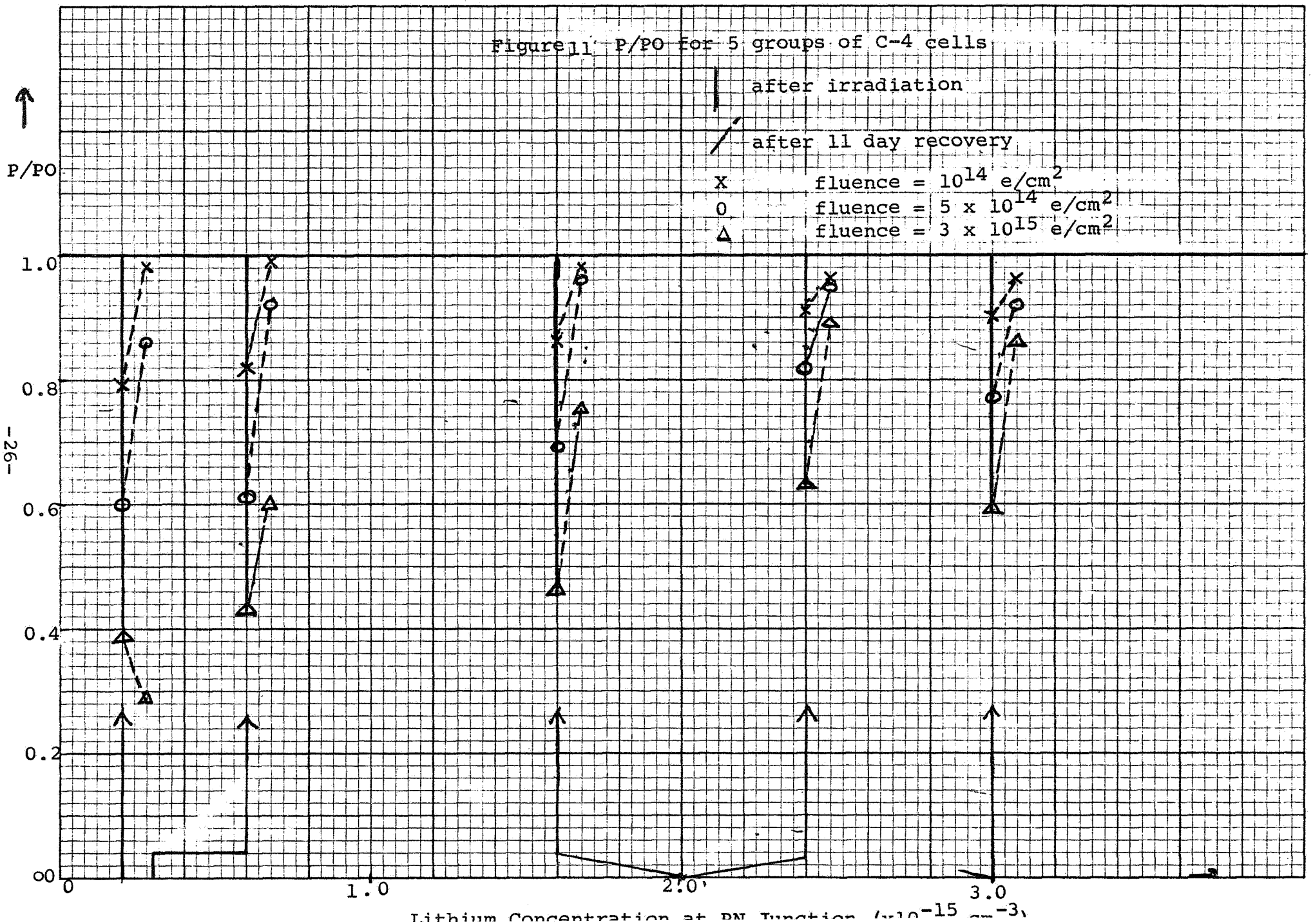

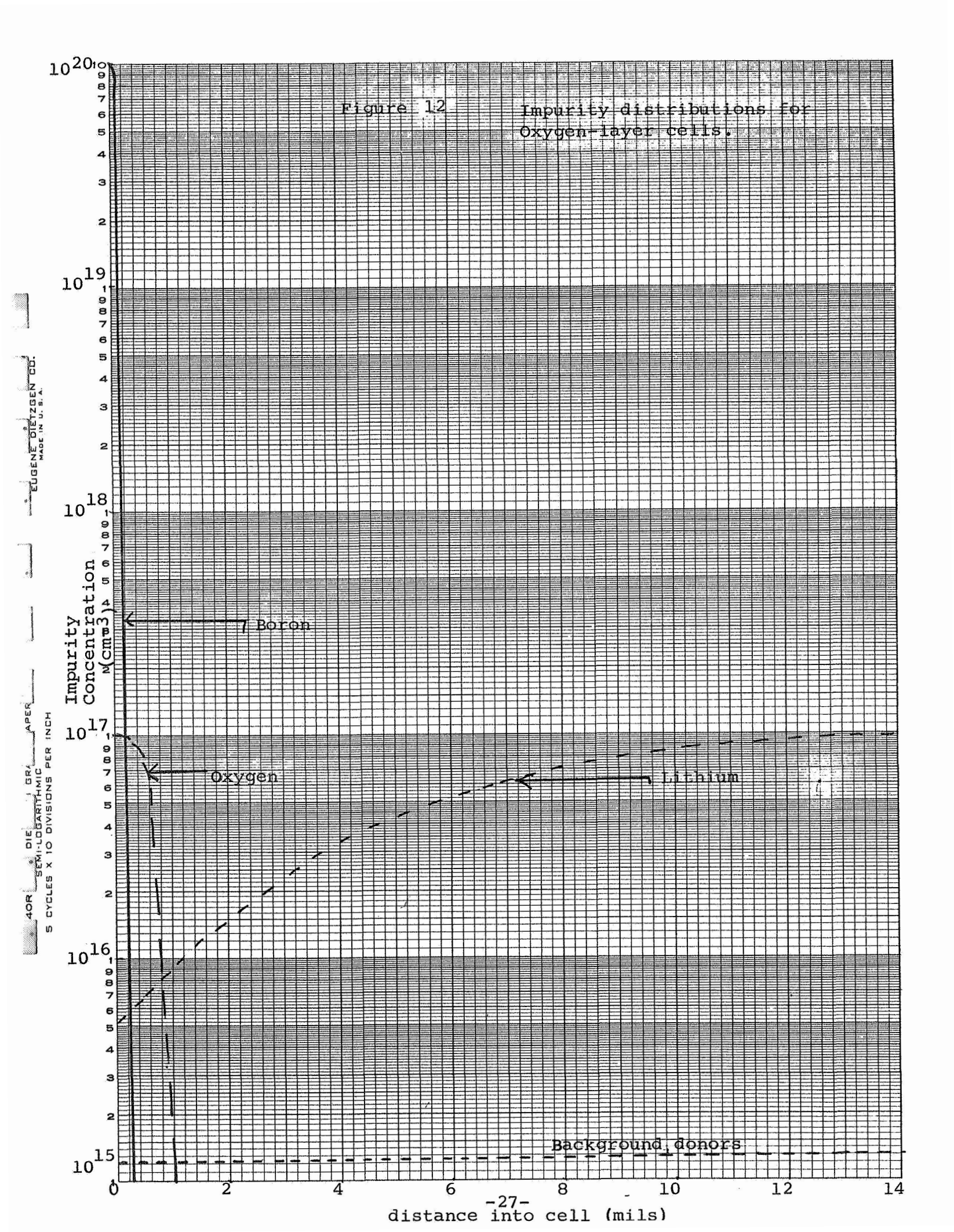
Figure 12
Impurity distributions for Oxygen-layer cells.
Impurity Concentration N(cm⁻³)
Boron
Oxygen
Lithium
Background donors
distance into cell (mils)
0
2
4
6
8
10
12
14
10^20
10^19
10^18
10^17
10^16
10^15

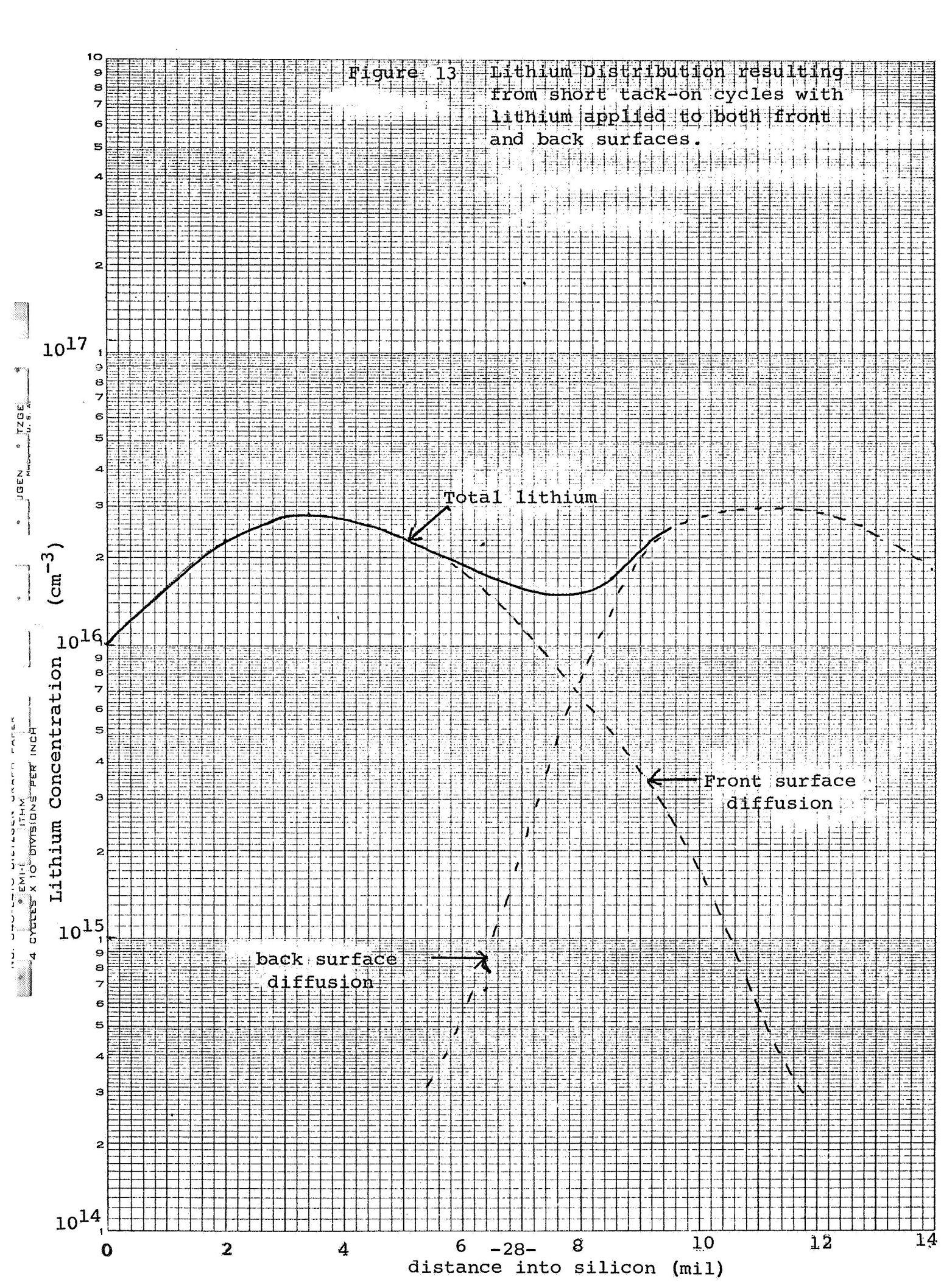
Figure 13 Lithium Distribution resulting from short tack-on cycles with lithium applied to both front and back surfaces.
Total lithium
Front surface diffusion
back surface diffusion
Lithium Concentration (cm^{-3})
distance into silicon (mil)
10^{17}
10^{16}
10^{15}
10^{14}
0
2
4
6
8
10
12
14